Title

SOBA: Development and testing of a soluble oligomer binding assay for detection of amyloidogenic toxic oligomers.

Journal

Proceedings of the National Academy of Sciences of the United States of America, 119(50)

Authors

Shea, Dylan

Colasurdo, Elizabeth

Smith, Alec

et al.

Publication Date

2022-12-13

DOI

10.1073/pnas.2213157119

Peer reviewed

PNAS RESEARCH ARTICLE | BIOPHYSICS AND COMPUTATIONAL BIOLOGY

SOBA: Development and testing of a soluble oligomer binding assay for detection of amyloidogenic toxic oligomers

Dylan Shea[a,b], Elizabeth Colasurdo[c], Alec Smith[d], Courtnie Paschall[b,e], Suman Jayadev[f], C. Dirk Keene[g], Douglas Galasko[h], Andrew Ko[e], Ge Li[i,j,k], Elaine Peskind[c,k], and Valerie Daggett[a,b,1]

Edited by Claudio Soto, The University of Texas Health Science Center at Houston, Houston, TX; received August 12, 2022; accepted October 17, 2022 by Editorial Board Member Angela M. Gronenborn

The formation of toxic Amyloid β-peptide (Aβ) oligomers is one of the earliest events in the molecular pathology of Alzheimer's Disease (AD). These oligomers lead to a variety of downstream effects, including impaired neuronal signaling, neuroinflammation, tau phosphorylation, and neurodegeneration, and it is estimated that these events begin 10 to 20 y before the presentation of symptoms. Toxic Aβ oligomers contain a nonstandard protein structure, termed α-sheet, and designed α–sheet peptides target this main-chain structure in toxic oligomers independent of sequence. Here we show that a designed α–sheet peptide inhibits the deleterious effects on neuronal signaling and also serves as a capture agent in our soluble oligomer binding assay (SOBA). Pre-incubated synthetic α–sheet-containing Aβ oligomers produce strong SOBA signals, while monomeric and β-sheet protofibrillar Aβ do not. α–sheet containing oligomers were also present in cerebrospinal fluid (CSF) from an AD patient versus a noncognitively impaired control. For the detection of toxic oligomers in plasma, we developed a plate coating to increase the density of the capture peptide. The proof of concept was achieved by testing 379 banked human plasma samples. SOBA detected Aβ oligomers in patients on the AD continuum, including controls who later progressed to mild cognitive impairment. In addition, SOBA discriminated AD from other forms of dementia, yielding sensitivity and specificity of 99% relative to clinical and neuropathological diagnoses. To explore the broader potential of SOBA, we adapted the assay for a-synuclein oligomers and confirmed their presence in CSF from patients with Parkinson's disease and Lewy body dementia.

alpha-sheet | toxic oligomer | SOBA | Alzheimer's disease | detection

Significance

Early detection and disease-modifying treatments are necessary to combat Alzheimer's disease. A first step in that process is early diagnosis to intervene before irreparable damage occurs, which is estimated to begin 10 to 20 y before the presentation of symptoms. The earlier discovery of α–sheet structure during conformational changes associated with amyloidogenesis led to a potential target for selective and early detection of these oligomers. Here we show that a de novo designed α–sheet peptide neutralizes the toxic effect of Aβ oligomers on neuronal signaling and serves as a capture agent for their detection. The presence of α–sheet Aβ oligomers in plasma, as detected with SOBA, is highly correlated with Alzheimer's disease.

Early diagnostics and disease-modifying therapeutics for Alzheimer's disease (AD) remain elusive (1). Amyloid plaques are pathological hallmarks of AD; however, there is increasing evidence that damage by toxic oligomers of the amyloid- β peptide (Aβ) begins much earlier, prior to amyloid plaque deposition (2–11). The presence of oligomers in the brains of transgenic mice and AD patients correlates with synaptic dysfunction and memory loss, while plaque burden does not (3, 5–7). Furthermore, the formation of toxic Aβ oligomers is the first known biochemical change during amyloidogenesis, preceding tau phosphorylation, plaque deposition, tau neurofibrillary tangle formation, and neurodegeneration (6–15).

The primary mode of premortem AD diagnosis is through clinical evaluation of symptomatic individuals (the black curve on the far *Right* in Fig. 1*A*) (16), but there is interest in establishing new biomarkers to provide earlier and more accurate diagnoses (17, 18). Moving to the *Left* in Fig. 1*A*, PET imaging of Aβ plaques and tau tangles inform and confirm clinical diagnoses, and decreasing levels of the 42-residue Aβ fragment (Aβ42) in CSF and plasma are associated with its deposition in plaques (19–21). The Aβ42/40 (ratio of concentrations of [Aβ42] to [Aβ40]) normalizes for inter-individual variability in peptide concentration and tends to outperform total [Aβ42] (22–24). In contrast, total tau and phosphorylated tau levels increase during AD (20, 25, 26). These biomarkers are not directly or uniquely correlated with toxicity or AD-specific neurodegeneration (27–29). Toxic Aβ oligomers form earlier in the disease process (Fig. 1*A*); however, their specific detection has thus far eluded researchers. The toxic oligomers represent a fraction of both the total Aβ and the total oligomer population (13, 30, 31), making their detection technically challenging. Additionally, it is difficult to selectively detect only the toxic oligomers rather than other conformational forms of Aβ42 (e.g., β-sheet-rich protofibrils, fibrils, or unstructured monomers).

Here we describe the selective targeting of toxic oligomers and the development of the soluble oligomer binding assay (SOBA), as well as proof-of-concept tests on banked cross-sectional and longitudinal AD plasma samples. We also tested CSF from patients with Parkinson's

Author contributions: D.S. and V.D. designed research; D.S. and A.S. performed research; E.C., C.P., S.J., C.D.K., D.G., A.K., G.L., E.P., and V.D. contributed new reagents/analytic tools; D.S., A.S., C.D.K., G.L., E.P., and V.D. analyzed data; and D.S., E.C., A.S., C.P., S.J., C.D.K., D.G., A.K., G.L., E.P., and V.D. wrote the paper.

Competing interest statement: The authors declare a competing interest. The authors have organizational affiliations to disclose. V.D. has a start up in this space, but the work reported here was performed at UW. V.D. and D.S. have stock in startup. V.D. and D.S. are inventors on a patent together and V.D. has other patents.

This article is a PNAS Direct Submission. C.S. is a guest editor invited by the Editorial Board.

[1]To whom correspondence may be addressed. Email: daggett@uw.edu.

This article contains supporting information online at https://www.pnas.org/lookup/suppl/doi:10.1073/pnas.2213157119/-/DCSupplemental.

Published December 9, 2022.

disease (PD) and Lewy body dementia (LBD) to address the broader potential of our technology. SOBA specifically targets toxic oligomers by utilizing α–sheet peptides complementary to the structure in the toxic oligomers in an enzyme-linked immunoassay (ELISA) format with the substitution of a synthetic, designed α–sheet peptide for the conventional capture antibody. The capture peptide binds to α–sheet structure in toxic oligomers and the SOBA signal is highly correlated with toxicity, R^2 = 0.94 (13). An antibody is used to determine the type of toxic oligomer bound. An anti-Aβ antibody is used for AD and an anti-α-synuclein antibody is used for PD and LBD. The resulting signal was quantified via chemiluminescence using an horseradish peroxidase-linked secondary antibody.

α–sheet is a nonstandard protein structure discovered in molecular dynamics (MD) simulations of a variety of amyloid-disease-associated proteins (33, 34). Amyloidogenic proteins and peptides unrelated by sequence, structure, and disease all formed α–sheet, and we proposed and subsequently demonstrated that it is the defining feature of the toxic soluble oligomers in several amyloid systems (32–37), including toxic Aβ42 oligomers (13). We reasoned that this structure may represent a unique target for early detection, and we designed stable, soluble, nontoxic α–sheet peptides to complement the α–sheet structure in the toxic species (35). The strands of the α–sheet hairpins were templated with alternating L- and D-amino acids to recapitulate the novel main-chain structure observed in the MD simulations ((33, 34) and references therein). This is a critical feature of our designs, as they exploit the unique features of α–sheet main-chain structure for complementary binding between the main chain of the de novo α–sheets and the α–sheet main chain structure in the oligomers independent of sequence. Thus, unlike antibody binding, discrimination is based on secondary structure not side chains. The best-scoring designs were synthesized and characterized to verify the predicted structure using a variety of methods (32, 35–37). The resulting peptides bind the toxic oligomers, neutralizing toxicity in in vitro cell assays and in AD animal models (13, 32, 35, 37). Unrelated mammalian and bacterial amyloid proteins have been shown to form α–sheet during amyloidogenesis (35–37). Furthermore, our synthetic α–sheet peptides inhibit amyloid formation in these different, unrelated systems via preferential binding of the α–sheet-containing toxic oligomers (13, 32, 34–38).

Earlier studies set the stage for the work presented here (see ref. 13 for details). To summarize the key points as they relate to the current study, we developed a protocol that allows for successive population of different conformers during the aggregation process. The low molecular weight oligomers contain a mix of hexamers and dodecamers. They contain α–sheet, they are cytotoxic, and they peak during the lag phase prior to β-sheet formation. The extent of α–sheet present, as determined by circular dichroism (CD) and indirectly through SOBA, is positively correlated with cytotoxicity. As such, SOBA provides a readout of the α–sheet containing toxic oligomers.

Targeting Aβ Toxic Oligomers with a Designed α–Sheet Peptide: Neutralization and Detection

To investigate the ability of our synthetic α–sheet designs to selectively target Aβ (the 42-residue form of the peptide) toxic oligomers, we evaluated their effect on neuronal signaling with and

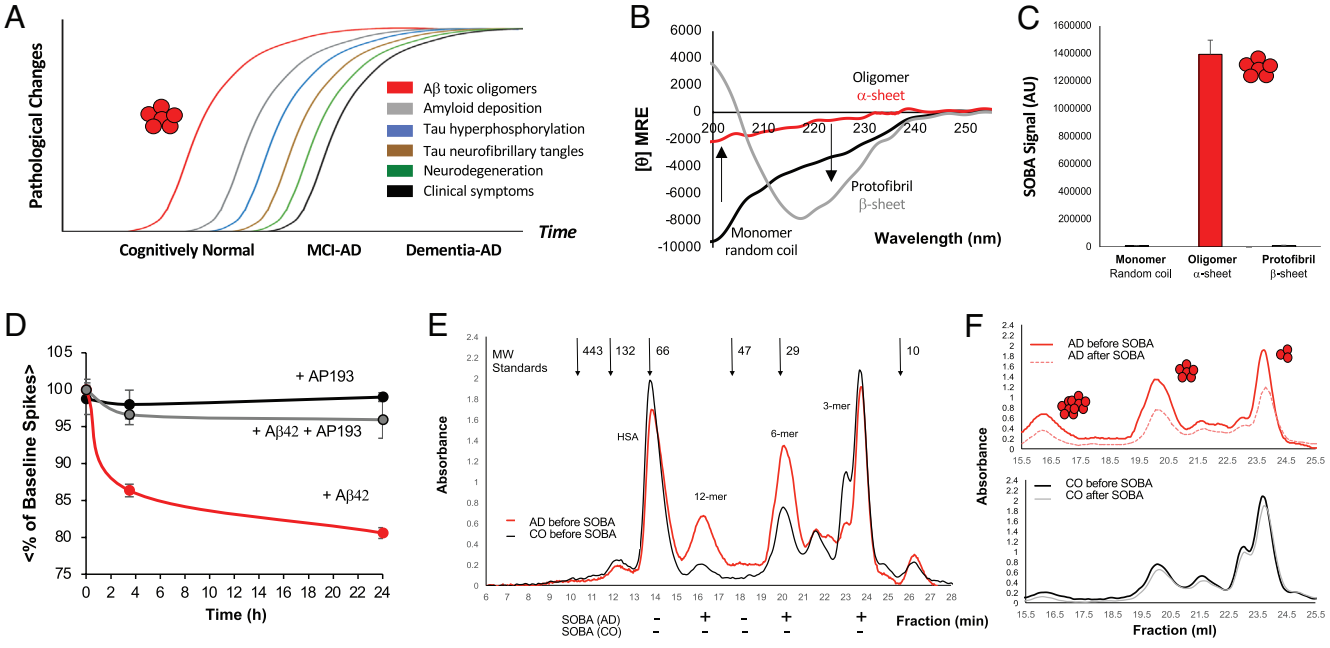

Fig. 1. Milestones in the molecular pathology of AD and targeting the toxic Aβ oligomers with a de novo designed α–sheet peptide. (*A*) Timing of different pathological milestones along the AD continuum. There is consensus regarding this general order of events (17–19), except that some studies and models put tau phosphorylation before Aβ plaque deposition. The Aβ oligomers are depicted in red as a hexamer, noting that hexamers and dodecamers (stacked hexamers) are the dominant α–sheet toxic oligomers (13) and they are approximately spherical by atomic force microscopy (32). (*B*) Structural changes in 75 μM Aβ42 in PBS during aggregation from unstructured monomer, to low-molecular-weight α–sheet soluble oligomers, to high-molecular weight β-sheet protofibrillar aggregates. Samples were diluted to 25 μM immediately before CD. (*C*) Preincubated Aβ42 samples in PBS (75 μM) spiked into plasma corresponding to the time points in panel *B* show that the α–sheet oligomers produced high SOBA signals while the monomer and β-sheet protofibrils did not (100 pM Aβ42 applied to SOBA in each case). (*D*) Effects of pre-incubated Aβ42 oligomers (75 μM in PBS, incubated for 24 h at 25 °C) on electrical activity of neuronal cells and maintenance of signal with co-administration of α–sheet design. Aβ42 oligomers (30 μM diluted in differentiation medium, see *Methods*) caused a 20% drop in the average number of spikes ($P < 0.002$ vs. other conditions). AP193 alone and Aβ42+AP193 (2:1, excess Aβ) were within the variability of what was observed in baseline measurements prior to adding compounds. (*E*) Size exclusion chromatograms (SEC) of neat human CSF on Superdex 200 column monitored at 254 nm. AD and CO control samples with assignments for peaks that are SOBA positive with three Aβ toxic oligomer peaks indicated, based on molecular weight standards. (*F*) Oligomer peaks for samples before and after SOBA, showing the depletion of 3-, 6-, and 12-mer peaks in the AD sample from binding of α–sheet oligomers and no change in these same peaks in the CO control sample.

without treatment with an α–sheet design (AP193). The α–sheet-containing oligomers were obtained by incubation of Aβ42 at neutral pH in phosphate-buffered saline (PBS), the α–sheet structure was confirmed by CD, and the dominant toxic species were hexamers and dodecamers, reproducing previous results (13). Aβ42 aggregation proceeds from an unstructured, "random coil" monomer, misfolds to α–sheet (as reflected in the relatively flat "null" spectrum) and then aggregates further and forms β-sheet structure (Fig. 1*B*). The alternating chirality of the amino acids forming the α–sheet leads to cancellation of the CD signals. Alternatively, one might think that mixture of random coil (negative signal) and β-sheet (positive signal) between 200 and 210 nm can lead to a null spectrum, as both random coil and β-sheet or Aβ42 are negative between 210 and 230 nm, and such a combination results in deeper negative curves that do not match the "null" CD spectra predicted and experimentally observed for α-sheet (*SI Appendix*, Fig. S1). Also, solution infrared experiments support the CD results, showing that the toxic Aβ42 oligomers adopt a structure distinct from that of the β-sheet protofibrils but indistinguishable from the spectra obtained for designed α–sheet peptides (13).

Samples from the three stages of the aggregation pathway were applied to SOBA using AP193 to capture the oligomers, and the α–sheet oligomers were preferentially detected with negligible binding of random coil monomers and β-sheet protofibrils (Fig. 1*C*). This selective binding is consistent with earlier results showing binding of a structurally well-characterized α–sheet design (AP407) to the hexameric and dodecameric oligomers, but not monomers by SEC, as well as nM affinity binding to the pure oligomers as measured by biolayer interferometry (13).

The Aβ42 oligomers were then applied to a network of differentiated neuroblastoma cells with functional neuronal signaling on a microelectrode array plate to evaluate the effect on their electrophysiology. Signaling, as reflected by the average number of spikes relative to baseline, dropped following application of the oligomers, while co-administration with AP193 maintained normal electrical activity (Fig. 1*D*). This indicates that AP193 targeted and neutralized the Aβ42 oligomers.

To explore targeting of Aβ oligomers in biological fluids, we performed size exclusion chromatography (SEC) of CSF from an AD patient and a noncognitively impaired control (CO) (Fig. 1*E*). The major SEC peaks are labeled for the expected Aβ42 oligomers based on molecular weight standards. The hexamer- and dodecamer-associated peaks were more pronounced in the AD sample, and they corresponded to the positions of toxic oligomers formed by synthetic Aβ42 in vitro (13). Furthermore, these CSF fractions tested positive for Aβ toxic oligomers with SOBA, in contrast to the peaks collected from the control (Fig. 1*E*). Comparison of the SEC traces of the original samples to the CSF remaining in the SOBA well after binding to the capture agent confirmed the preferential binding of Aβ hexamers and dodecamers in the AD subject (Fig. 1*F*). The coincidence of the CO curves before and after SOBA indicates that Aβ oligomers were not present. Interestingly, we also had a SOBA-positive peak in the AD CSF corresponding to a trimer, which was not observed with more concentrated synthetic Aβ42 oligomers (13).

These results demonstrate that AP193 binds the neurotoxic α–sheet oligomers and inhibits Aβ42-induced disruptions to synaptic signaling, and the same peptide captures Aβ oligomers in CSF. However, owing to the lower concentration of toxic oligomers in plasma, we developed a plate coating for increased display of our capture agent to amplify the signal for detection of Aβ oligomers in plasma (see *Methods* and associated *SI Appendix*, Fig. S2).

Detection of α–Sheet-Containing Aβ Oligomers in Plasma from MCI and AD Patients

We blindly tested 379 human plasma samples from 310 individuals classified based on a comprehensive clinical evaluation: CO (n = 221), MCI (n = 45), AD (n = 102), and other non-AD cognitive impairment (non-AD CI) (n = 11) (see *Methods* for detailed human subject descriptions). Of the CO cases, 11 were "converters" who progressed to MCI: 8 to MCI (AD-type) (n = 10, including 2 longitudinal samples) and 3 to non-AD CI in follow-up clinical visits. The 379 samples were considered independent for aggregate analyses.

The CO, MCI, and AD groups had similar mean ages, nearly equal distribution by sex, and 53% were at risk of AD based on their APOE4 genotype (*SI Appendix*, Fig. S3 and Table 1*A*). The Clinical Dementia Rating (CDR) and Mini Mental State Exam (MMSE) cognitive scores demonstrated progressive decline across CO ➞ MCI ➞ AD (Table 1*A* and *SI Appendix*, Fig. S3). There was a bimodal distribution of SOBA values in the CO group: 1) negative CO cases and 2) individuals with significant SOBA scores who later converted to MCI, which we refer to as preclinical AD, or PC-AD (Fig. 2*A*). SOBA provided good discrimination between the CO and MCI and AD participants, with a cutoff value of 28,207, as determined through a receiver operating characteristic analysis (ROC, presented below). Values above this cutoff were considered SOBA positive and values below were SOBA negative (Fig. 2*A* and Table 1*B*). The cutoff discriminating SOBA-positive and SOBA-negative samples was independently confirmed using an orthogonal method by determining the limit of quantification in plasma spiked with in vitro Aβ42 α–sheet containing oligomers. The signal was compared for toxic oligomer samples from 1 nM to 1 aM and blanks in which the AP193 capture peptide was not included (*SI Appendix*, Fig. S2).

The agreement between SOBA and the clinical diagnoses for the MCI and AD samples (n = 147) was excellent with only one discrepancy. In this case, the clinical diagnosis was AD, but the plasma SOBA value was low (12,323 ± 3503, subject ID = ID54, *SI Appendix*, Data File). The CDR and MMSE scores were indicative of mild–moderate dementia (CDR = 1, MMSE = 13). We cannot definitively determine whether SOBA or the clinical diagnosis is incorrect; neuropathological results are not available.

Plasma SOBA Levels and Neuropathological Diagnoses

Autopsies were performed on 62 of the 310 participants on average 5.7 y after their final assessment (range 0 to 16 y). Fifty-three of these cases exhibited AD neuropathology, 52 out of 53 of which had positive SOBA values, resulting in 98% of the neuropathologically confirmed AD cases being correctly detected by SOBA in samples from 1 to 13 y prior (average of 6 y). There was one discrepancy: The diagnosis based on the neuropathological findings was AD, but the SOBA value was low, and the original diagnosis was non-AD CI (ID103).

One of the "known" converters (ID60) had five annual clinical visits, and SOBA was positive for every visit. This participant was a 74-y-old female, *APOE-ε4/4* genotype who was diagnosed with MCI at the 4th and 5th visits and died less than a year later. The primary neuropathologic diagnosis was vascular brain injury with a cerebral amyloid angiopathy score of 3, as well as a contributing diagnosis of AD. Interestingly, one MCI case (ID16) with mild AD pathology (CERAD sparse neuritic plaque density, Braak stage III neurofibrillary tangle burden) had an elevated SOBA score (41,074 ± 3904) 10 y prior to death. These results suggest that

Table 1. (A) Subject characteristics for samples by clinical diagnosis and (B) Biomarker summaries for samples by clinical diagnosis

# Samples	CO (n = 221)	MCI (n = 45)	AD (n = 102)	Non-AD CI (n = 11)	Total (n = 379)
Panel A					
Age (years)					
Mean (SD)	63.4 (14.9)	72.7 (11.0)	69.6 (10)	66.5 (12.3)	71.8 (9.2)
Range	20–100	47–88	39–88	53–87	
Female	150 (68%)	17 (38%)	49 (48%)	6 (55%)	222 (58%)
CDR Score					
Range	0.0–0.5	0.0–1.0	0.5–3.0	0.0–3.0	0.0–3.0
MMSE Score					
Mean (SD)	29.2 (1.3)	26.9 (2.4)	21.1 (5.6)	24.9 (5.9)	26.0 (5.0)
Range	26–30	22–30	4–30	15–30	
Panel B					
Plasma SOBA $A\beta_{toxic\text{-}oligomers}$ Signal					
Mean (SD)	16,089 (6,578)	58,192 (21,233)	68,606 (35,289)	14,538 (2,200)	43,367 (28,729)
Range	3,582–42,982	36,171–126,897	12,323–250,536	11,685–18,014	
CSF [Aβ42]					
Mean (SD)	318 (158)	245 (149)	211 (98.6)	275 (141)	232 (134)
Range	69–1014	3–747	49–519	69–535	
CSF [Tau]					
Mean (SD)	50 (20.3)	102 (68.0)	77 (35.8)	45 (9.1)	72 (53.5)
Range	18–170	42–337	32–271	30–63	
CSF [p-Tau181]					
Mean (SD)	34 (17.5)	94 (63.3)	56 (33.5)	24 (5.3)	54 (43.1)
Range	12–140	29–271	26–216	20–39	

These entries correspond to individual samples, not participants, and as such, the diagnoses and other entries in the tables can change for an individual over time and are provided in aggregate here. Individual breakdowns and analyses by subjects as opposed to samples are provided in the *SI Appendix* and discussed in the text. The full data set from which these values were calculated is provided in the *SI Appendix*, Data File.

SOBA can detect early AD pathology. The remaining nine autopsy diagnoses were normal and other non-AD CI (described further below), and eight out of nine were SOBA negative, while one was a SOBA-positive frontotemporal lobar degeneration, FTLD, case (ID27).

Preclinical Detection of Aβ Oligomers in Controls Prior to Progression to MCI

All eight known participants who converted from CO to MCI were SOBA positive prior to conversion, with signals comparable to those of MCI and AD cases. Three other CO controls tested SOBA positive, and the clinical archives contained follow-up visits for 2 of the 3. In the first case, the plasma sample was from the participant's first visit in 2002 (SOBA = 40,327 ± 2,305) when the CDR and MMSE scores were 0 and 30, respectively, but they progressed to 0.5/28 in 2007 (participant ID69). In the second case, the SOBA score was elevated (39,761 ± 10,771) in a CO control more than 95 y of age who underwent an autopsy 2 y later (ID61). The autopsy revealed mild AD neuropathologic change (CERAD = sparse and Braak stage = III/VI). While these scores did not meet the criteria for AD (intermediate or high likelihood), they confirmed the SOBA prediction of PC-AD.

For comparison, the conventional CSF biomarkers (Aβ42, Aβ42/40, tau, p-tau181 and combinations thereof) exhibited significant overlap, making it difficult to distinguish CO from MCI/AD (Figs. 2 *B*–*F*). Furthermore, the confirmed PC-AD cases were also indistinguishable from the controls. The identification of SOBA-positive controls who progressed to MCI supports the idea that the toxic oligomers may provide an early window into PC-AD (Fig. 2*G*). As an example, consider two cognitively unimpaired controls (Fig. 2*H*). One was an 80-y-old male with normal CDR and MMSE scores, normal CSF biomarker, and plasma SOBA levels, and *APOE-ε3/3* genotype, i.e., not at risk. The other was very similar: 82-y-old male, *APOE-ε3/3,* and normal CSF biomarker levels; however, his SOBA level was high, and he progressed to MCI 4 y later.

Longitudinal SOBA Values and Predicting Conversion to MCI

Of the 310 individuals, 59 had at least one follow-up visit with samples evaluated by SOBA. Each of the SOBA-positive CO controls with follow-up records eventually converted to MCI and had elevated SOBA signals prior to clinical diagnosis of MCI (Fig. 3*A*), suggesting that high preclinical SOBA scores are associated with an elevated risk of progression to MCI. The SOBA scores did not change appreciably in most cases as the disease progressed, consistent with a dynamic quasi-equilibrium of Aβ toxic oligomers being produced and cleared or deposited into plaques. The CO controls below the SOBA threshold remained low and either retained CO status or converted to non-AD CI. Some samples with entry diagnoses of MCI displayed increased SOBA scores with time while others did not, but they all remained SOBA positive (Fig. 3*A*). To put the extent of the changes observed in perspective, the largest correspond to a change of ~5 fM, and these,

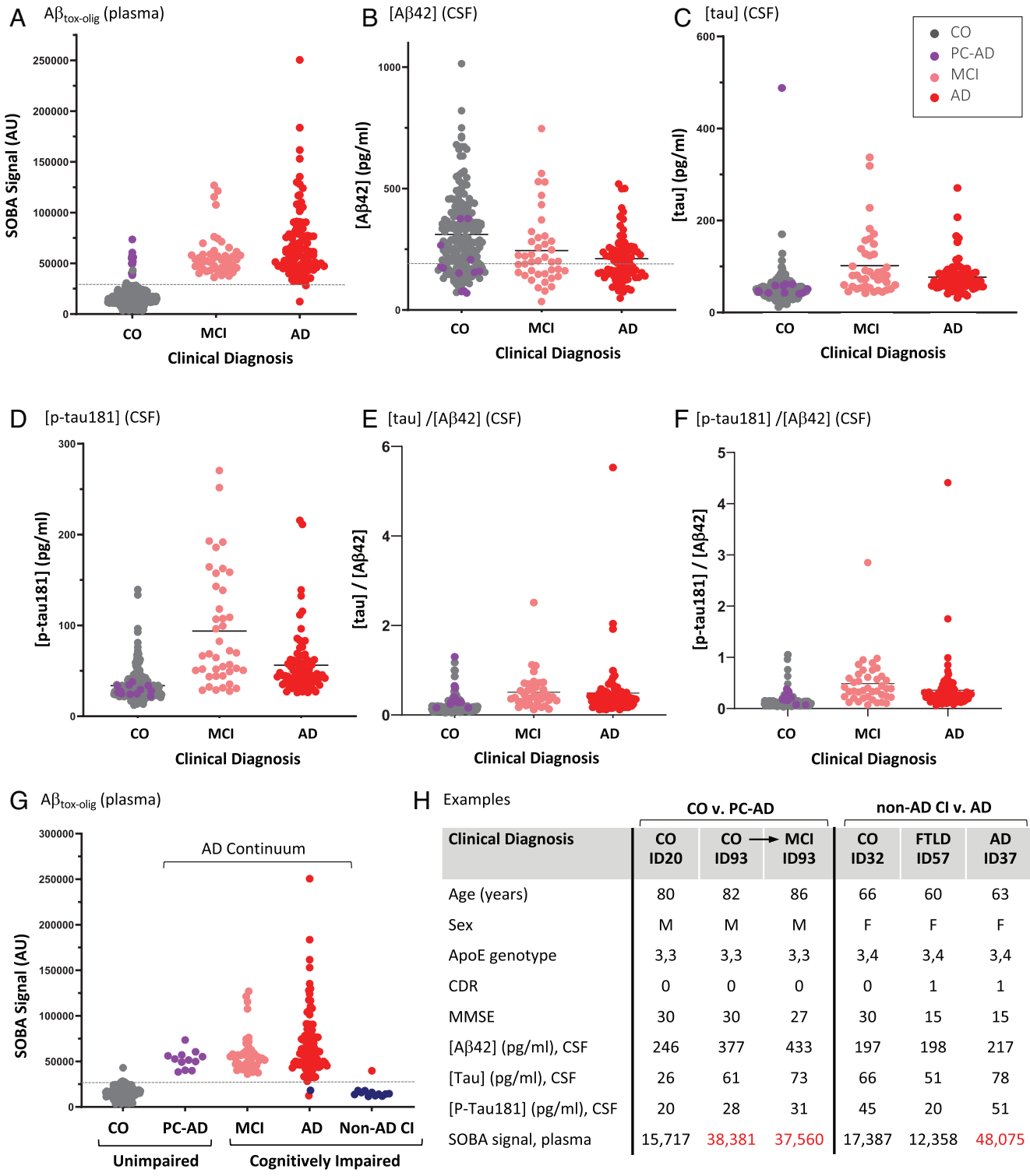

H Examples

	CO v. PC-AD			non-AD CI v. AD		
Clinical Diagnosis	**CO ID20**	**CO ID93**	**CO → MCI ID93**	**CO ID32**	**FTLD ID57**	**AD ID37**
Age (years)	80	82	86	66	60	63
Sex	M	M	M	F	F	F
ApoE genotype	3,3	3,3	3,3	3,4	3,4	3,4
CDR	0	0	0	0	1	1
MMSE	30	30	27	30	15	15
[Aβ42] (pg/ml), CSF	246	377	433	197	198	217
[Tau] (pg/ml), CSF	26	61	73	66	51	78
[P-Tau181] (pg/ml), CSF	20	28	31	45	20	51
SOBA signal, plasma	15,717	38,381	37,560	17,387	12,358	48,075

Fig. 2. SOBA discriminates between controls, non-AD CI, and MCI/AD cases. (*A*) Aβ toxic oligomers detected with SOBA plotted for plasma samples (n = 379) and colored by clinical diagnosis (see legend at right). SOBA-positive CO samples correspond to false positives or preclinical AD "converters," PC-AD, which are colored purple if validated through clinical follow-up or autopsy. Averages of raw luminescent readings are provided. Samples with signals above the threshold (28,207 signal, denoted by the dashed horizontal line) are SOBA positive and those below are SOBA negative. (*B–F*) Plots for the CSF biomarkers associated with the plasma samples in panel *A*: Aβ42, tau, p-tau181, tau/Aβ42, and p-tau181/Aβ42, respectively, were determined using commercial Luminex and/or InnoGenetics multiplex assays. Note overlap between the CO, MCI, and AD groups as well as the lack of discrimination between PC-AD and CO cases. (*G*) SOBA values (n = 379) binned by final diagnosis but colored by original clinical diagnosis. Neuropathological diagnoses were used when available, clinical otherwise. The toxic oligomer-positive, SOBA-positive CO cases correspond to an early preclinical stage along the AD continuum. The non-AD CI cases are also included. Note the 3 cases contrary to the final diagnoses determined with neuropathological and biomarker follow up. Two are SOBA-negative with one clinically diagnosed as AD (red) and the other clinically diagnosed as non-AD CI (blue) but determined to be AD from the neuropathological assessment. The other is a SOBA-positive case that was determined to be non-AD CI by autopsy. (*H*) Case studies of CO versus PC-AD (CO → MCI converters) and non-AD CI versus AD. CO v. PC-AD: Comparison of biomarker levels between two individuals (ID20 and ID93) in the control group and the values when ID93 later converted to MCI. AD v. non-AD CI and CO: Case study of two cognitively impaired individuals diagnosed with dementia, one due to AD (ID37) and the other FTLD (ID57), representing a non-AD case of cognitive impairment. A control CO subject is provided for reference (ID32).

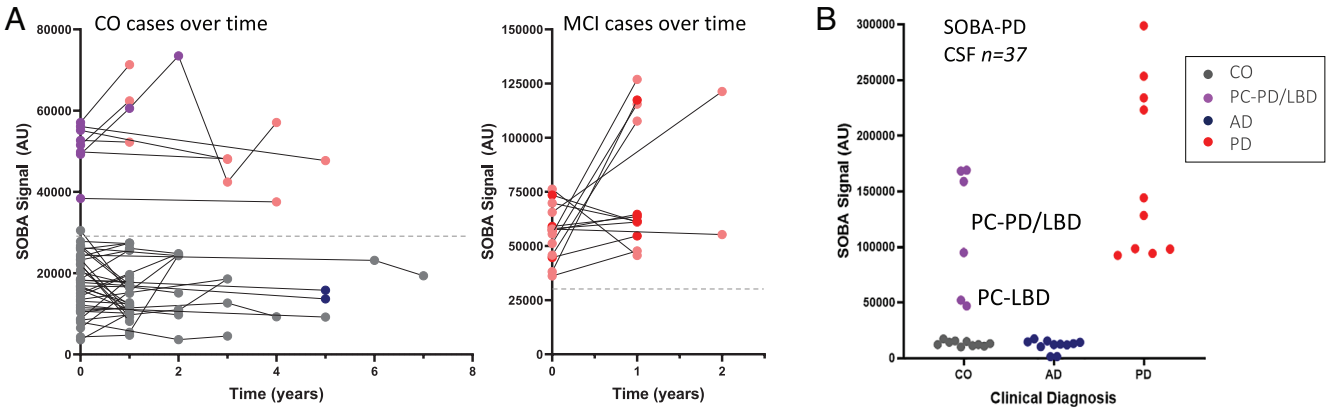

C

	ID73				ID21		
Clin Dx	CO	Other	PD/LBD		CO	MCI-AD	PD/LBD
Path Dx				PD/LBD			
SOBA-PD	+	+			+	+	
SOBA-AD	-	-			+	+	
Age (yrs)	82	87	88	90	77	80	84

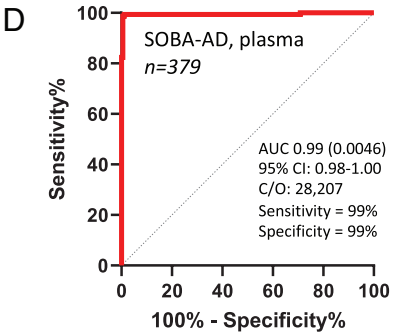

Fig. 3. SOBA Aβ toxic oligomer signals over time, overall performance in distinguishing controls (CO) and non-AD dementia participants from those on the Alzheimer's Disease continuum (PC-AD, MCI, and AD), and extension of the assay to detect α–synuclein toxic oligomers associated with PD and Lewy body disorders. (*A*) Profile plot of SOBA-AD signals for longitudinal samples separated by clinical diagnosis at study entry and change in diagnosis over follow up for 59 participants with at least one follow-up visit. Note the difference in the scales of the y-axes. (*B*) SOBA results for CSF from patients with PD and/or LBD patients and controls with a modified version of the assay that replaces the 6E10 Aβ detection antibody for the 4B12 a-synuclein antibody (SOBA-PD). CSF was diluted 1:10 in PBS. The purple values correspond to four CO individuals (two of which had two samples each, see panel *C*) from the AD plasma sample set who were later diagnosed with PD and/or LBD. (*C*) Using SOBA-AD and SOBA-PD for discrimination of AD and PD/LBD, potential comorbidity, and preclinical detection of PD/LBD for two CO controls from the AD plasma set who later converted to PD. SOBA-PD detected a-synuclein toxic oligomers in the CSF 6 and 7 y, respectively, before clinical diagnosis. In addition, one of the subjects also tested positive for Aβ toxic oligomers by SOBA-AD (plasma), suggesting potential comorbidity. Furthermore, two CO cases were later found to have LBD upon autopsy 13 and 16 y later. Their CO CSF samples were SOBA-PD positive. (*D*) Receiver operating characteristic analysis and associated results for SOBA-screened plasma in this study, n = 379 samples. Comparison was made against the neuropathology diagnoses where available and confirmed clinical diagnoses when not (confirmed = follow-up including neuropsychological and biomarker assessments). Further comparisons are provided in the *SI Appendix*, Data set.

in turn, are approximately four orders of magnitude lower than the total concentration of Aβ42 in the CSF.

SOBA Discriminates AD from Other Neurodegenerative Diseases

In addition to the MCI and AD cases, there were 11 participants who were clinically diagnosed with non-AD CI, all of whom had low, negative SOBA scores (Fig. 2*G*). Two were clinically diagnosed with Huntington's disease, four with FTLD, one with progressive supranuclear palsy (PSP), one with PD, and the remaining three were classified as other non-AD dementia (unknown cause). Three of these were originally in the CO group and converted to non-AD CI with low SOBA scores indistinguishable from previous CO values (Fig. 3*A*). In addition, three more cases of LBD were identified during autopsy. Two were in the CO group (ID67 and ID78), and the third was initially clinically diagnosed as PSP. These findings illustrate the potential for SOBA in differential diagnosis (see Fig. 2*H* for specific example).

SOBA captures α–sheet toxic oligomers based on structure, not sequence, and a detection antibody is used to identify the chemical nature of the bound oligomers via sequence. Thus, SOBA is modular by design: The anti-Aβ antibody used on the plasma samples (now referred to as SOBA-AD) can be replaced by antibodies specific for other amyloid proteins. As an initial proof of principle, we tested CSF from 10 PD patients undergoing deep brain stimulation surgery, with an anti-α-synuclein antibody (SOBA-PD). We obtained strong SOBA signals and good discrimination between PD patients and CSF from AD and CO individuals from the AD plasma study (Fig. 3*B*). The CO samples were both SOBA-AD and SOBA-PD negative, while the AD cases were SOBA-AD positive but SOBA-PD negative.

Two controls from the AD study were later diagnosed with PD/LBD. PD and LBD labels reflect symptoms, but they are both α–synucleopathies and detected by SOBA-PD (2 samples from each) (Fig. 3*B*). In one case (ID73), the individual tested positive as a CO control, 8 y prior to the autopsy diagnosis of PD/LBD and was negative by SOBA-AD (Fig. 3*C*). In the other case (ID21), the SOBA-PD score was positive 7 y prior to the clinical diagnosis of PD/LBD; however, this individual also tested positive by SOBA-AD (Fig. 3*C*), suggesting the possibility of comorbidity. In addition, the two CO subjects (ID67, ID78) with neuropathological diagnoses of LBD tested positive with SOBA-PD from samples 16 and 13 y before the autopsies.

SOBA Performance

ROC analyses were performed to assess the ability of SOBA to distinguish MCI and AD from CO. This technique determines the cutoff providing the highest sensitivity and specificity given a

particular gold standard or reference. Fig. 3*D* used the neuropathological diagnoses plus the clinical diagnoses when autopsies were not available, resulting in 99% sensitivity and 99% specificity (n = 379, considering each sample as an independent assessment). Of note, 67% of the clinical diagnoses were biomarker confirmed based on the CSF Aβ42 concentration: CO > 192 pg/ml and MCI/AD < 192 pg/ml. The remaining 33% of the plasma samples were CSF biomarker/clinical diagnosis discordant, yet SOBA demonstrated good agreement with the clinical diagnoses independent of [Aβ42]. An important contributing factor to the performance of SOBA is the lack of overlap between: 1) controls and those on the AD continuum, including PC-AD, and 2) AD and non-AD dementias. The determination of *P*-values comparing the mean SOBA values binned by clinical diagnosis, resulted in two clear groups: CO and non-AD CI samples were indistinguishable, and the samples on the AD continuum (PC-AD, MCI, AD) were indistinguishable (*SI Appendix*, Fig. S4). In contrast, the *P*-values between the two groups were highly significant ($P < 10^{-7}$). The results from the SOBA ROC analyses were similar for different reference diagnoses (clinical, neuropathological, and combined) on both a sample and subject basis, and the results for the CSF biomarkers are provided for comparison (*SI Appendix*, Figs. S5, S6 and Table S1). SOBA was uncorrelated with the total CSF Aβ42 content and independent of age and ApoE4 status (*SI Appendix*, Fig. S7).

Concluding Remarks

SOBA specifically detects α–sheet containing toxic oligomers—critical early players in the molecular pathology of AD and other amyloid diseases. These Aβ oligomers were detected in MCI and AD patients in plasma using a de novo-designed α–sheet capture agent. Furthermore, SOBA-AD detected the oligomers in non-cognitively impaired controls years before converting to MCI, suggesting that it may provide standalone, preclinical detection of AD. Moreover, SOBA-AD discriminated AD from other forms of dementia and the non-AD forms of dementia can be identified using different detection antibodies in SOBA. As an example, we created SOBA-PD, which identified both active and preclinical PD and LBD cases, albeit the number of samples is small. SOBA is not reliant on invasive sample collection procedures, multistep processing and enrichment, sophisticated proprietary equipment, patient information, advanced analytics with combinations of parameters to optimize discrimination, or inclusion of risk factors, making it potentially easy to deploy in standard labs and clinics. Here we describe the technology and provide proof of concept in an exploratory study on a small number of samples. Future studies will be pursued to replicate, validate and extend these findings by screening more diverse samples from a variety of sources.

Methods

The capture peptide, AP193, for the SOBA assay and electrophysiology experiments was produced by manual solid-phase peptide synthesis and microwave peptide synthesis (CEM, Liberty Blue). Aβ42 used in the experiments and as an oligomer standard for SOBA was obtained from the ERI Amyloid Laboratory (Oxford, CT). The oligomer standards were prepared based on protocols described previously (13). Size exclusion chromatography was performed using a Superdex 200 Increase 10/300 GL column on an AKTA Pure System (GE Life Sciences). The various steps, sample preparation, and antibodies used for the SOBA experiments are described in detail in *SI Appendix*. The AD study was approved by the UW institutional review board (IRB; under approval numbers 01-8926-V and 01173). All participants, or their legally authorized representative in the case of AD and other dementia participants, provided written informed consent prior to any study procedures. The PD study was approved by the UW IRB (STUDY00009130). A detailed description of the different methods employed is provided in the *SI Appendix*.

Data, Materials, and Software Availablity. All study data are included in the article and/or *SI Appendix*.

ACKNOWLEDGEMENTS. We are grateful for financial support from the National Institute of Aging (1R01AG067476 to V.D.) and (P01 05136 to E.P.), the National Institute of Health Bioengineering and Cardiovascular Training Grant (NIH/NIBIB 532EB1650 to D.S., M. Regnier P.D.), the Washington Research Foundation (to V.D.), and the Northwest Mental Illness Research, Education, and Clinical Center (to E.P.).

Author affiliations: [a]Molecular Engineering Program, University of Washington, Seattle, WA 98105; [b]Department of Bioengineering, University of Washington, Seattle, WA 98105; [c]Veterans Affairs Northwest Network Mental Illness Research, Education, and Clinical Center, Veteran Affairs Puget Sound Health Care System, Seattle, WA 98108; [d]Department of Physiology and Biophysics, University of Washington, Seattle, 98105; [e]Department of Neurosurgery, University of Washington, Seattle, WA 98195; [f]Department of Neurology, University of Washington, Seattle, WA 98195; [g]Department of Laboratory Medicine and Pathology, University of Washington, Seattle, WA 98195; [h]Department of Neurosciences, University of California, San Diego, La Jolla, CA 92093; [i]Mental Illness Research, Education and Clinical Center Veterans Affairs Puget Sound Health Care System, Seattle, WA 98108; [j]Geriatric Research, Education, and Clinical Center, Veterans Affairs Puget Sound Health Care System, Seattle, WA 98108; and [k]Department of Psychiatry and Behavioral Sciences, University of Washington, Seattle, WA 98195

1. Alzheimer's Association, Alzheimer's disease facts and figures.https://www.alz.org/media/Documents/alzheimers-facts-and-figures.pdf, https://www.alz.org/alzheimers-dementia/facts-figures (2022). Accessed 26 November 2022.
2. D. J. Selkoe, J. Hardy, The amyloid hypothesis of Alzheimer's disease at 25 years. *EMBO Mol. Med.* **8**, 595–608 (2016).
3. E. N. Cline, M. A. Bicca, K. L. Viola, W. L. Klein, The amyloid-beta oligomer hypothesis: Beginning of the third decade. *J. Alz. Dis.* **64**, S567–S610 (2018).
4. S. Li, D. J. Selkoe, A mechanistic hypothesis for the impairment of synaptic plasticity by soluble Abeta oligomers from Alzheimer's brain. *J. Neurochem.* **154**, 583–597 (2020).
5. J. L. Tomic, A. Pensalfini, E. Head, C. G. Glabe, Soluble fibrillar oligomer levels are elevated in Alzheimer's disease brain and correlate with cognitive dysfunction. *Neurobio. Dis.* **35**, 352–358 (2009).
6. A. Y. Hsia *et al.*, Plaque-independent disruption of neural circuits in Alzheimer's disease mouse models. *Proc. Natl. Acad. Sci. U.S.A.* **96**, 3228–3233 (1999).
7. T. Tomiyama, H. Shimada, APP Osaka mutation in familial Alzheimer's Disease–Its discovery, phenotypes, and mechanism of recessive inheritance. *Int. J. Mol. Sci.* **21**, 1413 (2020).
8. Oddo *et al.*, Triple-transgenic model of Alzheimer's disease with plaques and tangles: Intracellular Abeta and synaptic dysfunction. *Neuron* **39**, 409–421 (2003).
9. F. G. DeFelice *et al.*, Alzheimer's disease-type neuronal tau hyperphosphorylation induced by Abeta oligomers. *Neurobio. Aging* **29**, 1334–1347 (2008).
10. F. Amar *et al.*, Amyloid-beta oligomer Aβ*56 induces specific alterations of tau phosphorylation and neuronal signaling. *Sci. Signal.* **10**, eaal2021 (2017).
11. H. Zempel, E. Thies, E. Mandelkow, E.-M. Mandelkow, Abeta oligomers cause localized Ca2+ elevation, missorting of endogenous tau into dendrites, tau phosphorylation, and destruction of microtubules and spines*J. Neurosci.* **30**, 11938–11950 (2010).
12. T. Kim *et al.*, Human LilrB2 is a beta-amyloid receptor and its murine homolog PirB regulates synaptic plasticity in an Alzheimer's model. *Science* **341**, 1399–1404 (2013).
13. D. Shea *et al.*, α-Sheet secondary structure in amyloid β-peptide drives aggregation and toxicity in Alzheimer's disease. *Proc. Natl., Acad. Sci. U.S.A.* **116**, 8895–8900 (2019).
14. C. R. Jack Jr., *et al.*, Tracking pathophysiological processes in Alzheimer's disease: An updated hypothetical model of dynamic biomarkers. *Neurology* **12**, 207–216 (2013).
15. S. E. Counts, M. D. Ikonomovic, N. Mercado, I. E. Vega, E. J. Mufson, Biomarkers for the early detection and progression of Alzheimer's Disease. *Neurother.* **14**, 35–53 (2017).
16. M. N. Sabbagh, L.-F. Lue, D. Fayard, J. Shi, Increasing precision of clinical diagnosis of Alzheimer's disease using a combined algorithm incorporating clinical and novel biomarker data. *Neurol. Therapy* **6**, S83–S95 (2017).
17. K. Blennow, A review of fluid biomarkers for Alzheimer's disease: Moving from CSF to blood. *Neurol. Ther.* **6**, S15–S24 (2017).
18. B. Dubois *et al.*, Advancing research diagnostic criteria for Alzheimer's disease: The IWG-2 criteria. *Lancet Neurol* **13**, 614–629 (2014).
19. P. D. Mehta *et al.*, Plasma and cerebrospinal fluid levels of amyloid beta proteins 1–40 and 1–42 in Alzheimer disease. *Arch. Neurol.* **57**, 100–105 (2000).
20. A. Nabers, H. Hafermann, J. Wiltfang, K. Gerwert, Abeta and tau structure-based biomarkers for a blood- and CSF-based two-step recruitment strategy to identify patients with dementia due to Alzheimer's disease. *Alzheimer Dement. Diag. Assess. Dis. Mon.* **11**, 257–263 (2019).
21. S. Janelidze *et al.*, Plasma beta-amyloid in Alzheimer's disease and vascular disease. *Sci. Rep.* **6**, 26801 (2016).
22. I. Baldeiras *et al.*, Addition of the Abeta42/40 ratio to the cerebrospinal fluid biomarker profile increases the predictive value for underlying Alzheimer's disease dementia in mild cognitive impairment. *Alz. Res. Ther.* **10**, 33 (2018).
23. S. E. Schindler *et al.*, High-precision plasma beta-amyloid 42/40 predicts current and future brain amyloidosis. *Neurol.* **93**, e1645–e1659 (2019).

24. O. Hansson, S. Lehmann, M. Otto, H. Zetterberg, P. Lewczuk, Advantages and disadvantages of the use of the CSF amyloid beta 42/40 ratio in the diagnosis of Alzheimer's Disease. *Alz. Res. & Ther.* **11**, 34 (2019).
25. S. Palmqvist *et al.*, Discriminative accuracy of plasma phosphor-tau217 for Alzheimer disease vs other neurodegenerative disorders. *J. Am. Med. Assoc.* **324**, 772–781 (2020).
26. N. R. Barthelemy, K. Horie, C. Sato, R. J. Bateman, Blood plasma phosphortylated-tau isoforms track CNS change in Alzheimer's disease. *J. Exp. Med.* **217**, e20200861 (2020).
27. H. Vanderstichele *et al.*, Standardization of measurement of beta-amyloid (1–42) in cerebrospinal fluid and plasma. *Amyloid Int. J. Exp Clin. Invest.* **7**, 245–258 (2000).
28. B. Olsson *et al.*, CSF and blood biomarkers for the diagnosis of Alzheimer's disease: A systematic review and meta-analysis. *Lancet Neurol.* **15**, 673–684 (2016).
29. S. K. Herukka *et al.*, Recommendations for cerebrospinal fluid Alzheimer's disease biomarkers in the diagnostic evaluation of mild cognitive impairment. *Alzheimers Dement.* **13**, 285–295 (2017).
30. W. Hong *et al.*, Diffusible, highly bioactive oligomers represent a critical minority of soluble Aβ in Alzheimer's disease brain. *Acta. Neuropath.* **136**, 19–40 (2018).
31. D. L. Brody, H. Jiang, N. Wildburger, T. J. Esparza, Non-canonical soluble amyloid-beta aggregates and plaque buffering: Controversies and future directions for target discovery in Alzheimer's disease. *Alz. Res. Ther.* **9**, 62 (2017).
32. N. Maris, D. Shea, A. Bleem, J. D. Bryers, V. Daggett, Chemical and physical variability in structural isomers of an L/D α-sheet peptide designed to inhibit amyloidogenesis. *Biochemistry* **57**, 507–510 (2018).
33. R. S. Armen, M. L. DeMarco, D. O. V. Alonso, V. Daggett, Pauling and Corey's alpha-pleated sheet structure may define the prefibrillar amyloidogenic intermediate in amyloid disease. *Proc. Natl. Acad. Sci. U.S.A.* **101**, 11622–11627 (2004).
34. V. Daggett, Alpha-Sheet: The toxic conformer in amyloid diseases? *Acc. Chem. Res.* **39**, 594–602 (2006).
35. G. Hopping *et al.*, Designed alpha-sheet peptides inhibit amyloid formation by targeting toxic oligomers. *eLife* **3**, e01681 (2014).
36. A. Bleem, R. Francisco, J. D. Bryers, V. Daggett, Designed alpha-sheet peptides suppress amyloid formation in Staphylococcus aureus biofilms. *Nature Biofilms Microbiomes* **3**, 16 (2017).
37. J. Kellock, G. Hopping, B. Caughey, V. Daggett, Peptides composed of alternating L- and D-amino acids inhibit amyloidogenesis in three distinct amyloid systems independent of sequence. *J. Mol. Biol.* **428**, 2317–2328 (2016).
38. N. Paranjapye, V. Daggett, De novo designed α-sheet peptides inhibit functional amyloid formation of *Streptococcus mutans* biofilms. *J. Mol. Biol.* **430**, 3764–3773 (2018).